



Hydrogen evolution reaction in the presence of WS₂/g-C₃N₄ nanocomposite as photocatalyst

Mahshid Farahi^{1,*}, Tayebeh shamspur¹, Ali Mostafavi¹ and Fariba Fathirad²

¹ Department of Chemistry, Faculty of Science, Shahid Bahonar University of Kerman, Iran

² Department of Nanotechnology, Graduate University of Advanced Technology, Kerman, Iran

Abstract.

Photoelectrochemical water splitting method under visible-light illumination has attracted a lot of attention from all the world because of global need for clean energy and removal of pollution. Due to strong mechanical, physicochemical stability and marvelous electronic features, graphitic carbon nitride is a suitable no metal photocatalyst for hydrogen generation reaction. But the issue of super recombination rate of charge carriers is a significant obstacle in the efficiency that should be considered. It seems that coupling g-C₃N₄ with metals can enhance the photocatalytic efficiency. In the present research, we checked out the function of tungsten disulfide coupled with graphitic carbon nitride (WS₂/g-C₃N₄) on a semiconductor fluorine-doped tin oxide (FTO) glass in the alkaline solution. The nanoparticles were prepared by proper hydrothermal and calcination approaches and investigated by XRD analysis. Electrochemical reviews were done to measure the catalytic performance of prepared catalyst in alkaline solution under light irradiation with electrochemical techniques. The desired synthesized photocatalyst showed the Tafel slope of 61 mV dec⁻¹ and appropriate durability in alkaline solution for hydrogen evolution reaction (HER) in the presence of visible light. The benefits of using this proper photocatalyst for hydrogen generation in industrial scale were Low hydrogen reduction overpotential, proper electrocatalytic durability and high electrochemical function.

Keywords: Water splitting, g-C₃N₄, Hydrogen evolution

1. Introduction

The enormous utilization of fossil fuel resources to advance human activities and industrial processes not only leads to environmental pollution problems but also increasing the energy crisis (Han et al., 2017. Jo et al., 2020). Over the past decades, hydrogen has been extensively studied as an energy carrier that also has a high energy density (Han et al., 2017., Wu & Zhang, 2011). On the other hand, photocatalytic technology is known as a perfect way to convert non-renewable solar energy into chemical energy (Ding et al., 2017., Xu et al., 2020). An effective action in the photocatalytic process is selection the appropriate high-efficiency photocatalyst. Unfortunately, many of photocatalysts are still far from the practical application level due to their inherent disadvantages, including photocorrosion, fast recombination rate of charge carriers, low ability to absorb visible light, and extremely high



manufacturing costs (Jo et al., 2020). The high chemical and thermal stability of graphitic nitride carbon can prevent photocorrosion in the photocatalytic reaction (He et al., 2020). However, the photocatalytic function of graphitic carbon nitride is limited because of the small special surface area, the rapid recombination of light-induced electron-hole pairs, the finite active sites and also the low quantum efficiency (Ding et al., 2017., Zeng et al. 2018). Therefore, various methods have been reported to modify graphitic carbon nitride and remove its limitations. Some of these methods include copolymerization, doping with metal and non-metal elements, and coupling with other semiconductors to form composites (Akple et al., 2015). Tungsten disulfide is a chemical compound of the family of transition metal dicalcogenides that has a graphene-like layered structure and its properties depend on the layer and differ from the properties of the materials in the bulk state. The most important features of tungsten disulfide are high surface area, sheet-like morphology, and so on (Ansari et al., 2018). Therefore, tungsten disulfide has good photocatalytic activity and has been reported as a suitable cocatalyst for graphitic carbon nitride (Lin et al., 2020., Yan et al. 2018).

2. Methods

2.1. Material

All chemical materials were purchased from Merck and used without further purification.

2.2 Synthesis of bare g-C₃N₄

Typically, 5 g of thiourea was putted into a covered alumina crucible in a vacuum tubular muffle furnace. Then, as the valve opened, high-purity argon gas flowed into the furnace. The sample was calcined at 550 °C for 2 hours. The resulting yellow powder was introduced as g-C₃N₄.

2.3 Synthesis of g-C₃N₄/WS₂

The g-C₃N₄ /WS₂ composite with sandwich structured was prepared via calcination method. Firstly, prepared WO₃ as tungsten precursor was added into 5 mL ethanol and dispersed by sonication for 5 min. Then thiourea was slowly added to the above solution and stirred until the ethanol was completely evaporated. After completely drying, the obtained powder was transferred to a crucible. This product was placed in a Vacuum furnace under high-purity Ar gas and calcinated at 550 °C. Finally, brownish-green g-C₃N₄/WS₂ powder with a sandwich structured was obtained.

2.4 Preparation of the working electrode:

FTO glasses in dimensions of 2 × 1 cm² was subjected to ultrasonic waves in methanol, ethanol and deionized water solutions for 30 minutes, respectively. After washing, the FTO pieces were heated in an oven at 200 °C. In order to achieve a homogeneous solution, 1 mg of the nanocatalyst was mixed with water and ethanol and subjected to ultrasonic waves. Then 5 µl of the catalyst suspension was placed on a square centimetre of the surface by drop coating method. The substrate was again placed in a furnace at 350 °C for 30 minutes to stabilize the catalyst on the cathode surface.



3. Results and Discussion

In Figure 1, the crystal structures and chemical composition of $g\text{-C}_3\text{N}_4$ and $g\text{-C}_3\text{N}_4/\text{WS}_2$ were studied by XRD patterns. According to figure (1a), two diffraction peaks for $g\text{-C}_3\text{N}_4$ were detected. The weaker peak at 13.3° corresponds to (100) plane, which is attributed to in-planar tri-s-triazine unit. The stronger peak at 27.5° is related to (002) crystal plane, which is attributed to the interlayer stacking of the aromatic systems (Lin et al., 2020, Ding et al. 2015). In addition, according to figure (1b) after adding of tungsten to $g\text{-C}_3\text{N}_4$, two peaks became manifest at 33.2° and 58.4° that, were assigned to (100) and (110) crystalline planes of WS_2 , respectively. As the amount of tungsten increases, the peaks of WS_2 became stronger, while the peaks of $g\text{-C}_3\text{N}_4$ are weakened. Also, the absence of observation (002) crystalline plane means synthesis of WS_2 with a few or monolayer structure (Zhou et al. 2019., Lin et al. 2020).

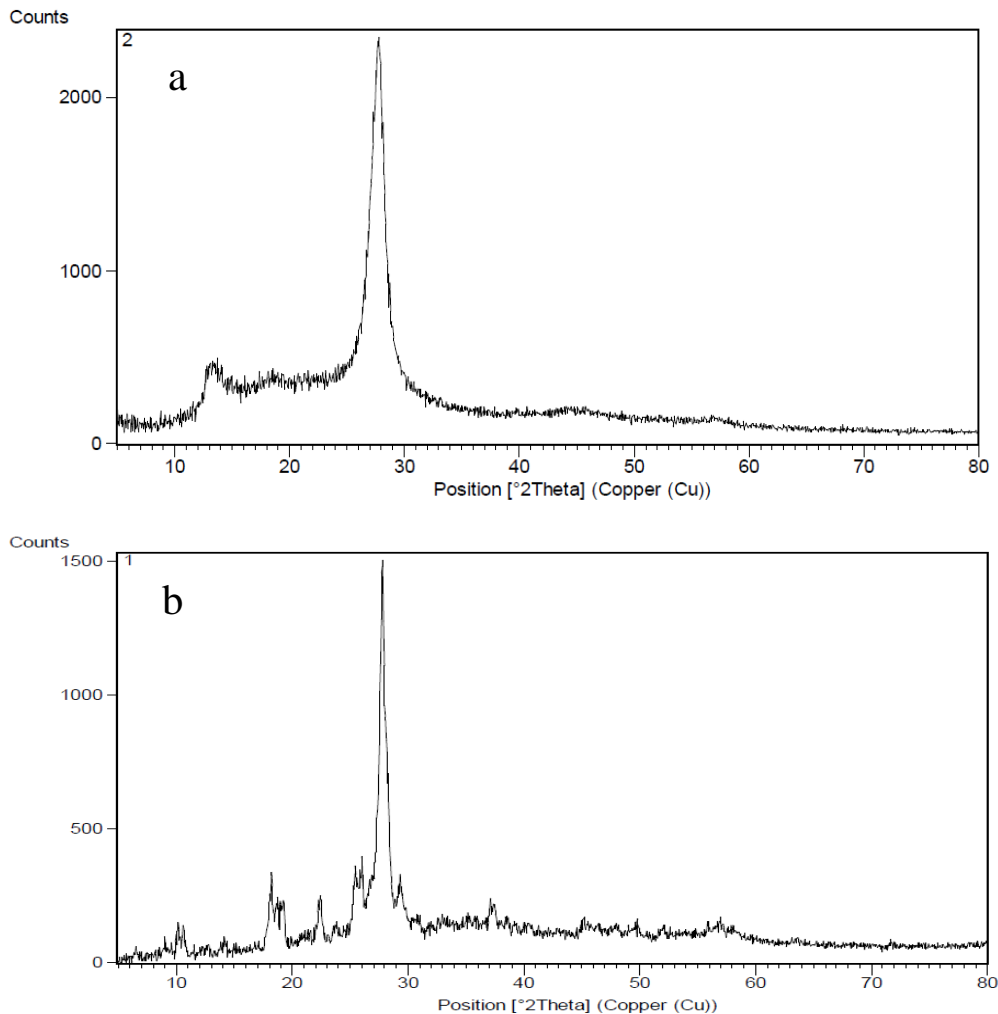


Figure 1: XRD patterns of the samples (a) $g\text{-C}_3\text{N}_4$, (b) $g\text{-C}_3\text{N}_4/\text{WS}_2$



3.1 Photo electrochemical measurements

Photoelectrochemical (PEC) measurements for investigation HER were performed in a quartz cell with the electrochemical station (PGSTAT 101, Eco Chemie, Netherlands) of the standard three-electrode system, which contained a Pt electrode as the counter electrode, Ag/AgCl electrode as the reference electrode and Fluorine Tin Oxide (FTO) glass as the working electrode. The photocurrent was measured in 0.5 M Na₂SO₄ supporting electrolyte solution and 0.5 V (vs. Ag/AgCl) bias potential was applied to the work electrode under irradiation of 300 W Xenon lamp as simulated sunlight. Before starting the test, a flow of N₂ gas was used for 30 min to remove air from electrolyte solution.

According to Table 1, when stack-layer WS₂ are embedded in g-C₃N₄ reduces transition of carriers in WS₂. As a result, the recombination of carriers increases. While the g-C₃N₄/WS₂, which are embedded monolayered WS₂ in g-C₃N₄, increases the separation of carriers. Another important parameter in photocatalytic performance is the amount of tungsten loaded. According to studies, 7.49 wt% WS₂/g-C₃N₄ showed the highest photocatalytic performance.

Sample	Morphology	wt% WS ₂	Photocatalyst performance
g-C ₃ N ₄ /WS ₂	sandwich	7.45	highest STH

4. Conclusion

In conclusion, g-C₃N₄/WS₂ nanocomposite were synthesized by hydrothermal and one-pot calcination methods. Then, we examined the synthesized nanocomposite as photoanode for hydrogen generation. The intense synergy between the components in g-C₃N₄/WS₂ nanocomposite that facilitate interfacial charge transfer to barrier the direct recombination of visible-light-induced electron-hole pairs, together with improved light absorption and specific surface area, contributed to the enhancement catalytic efficiency of the g-C₃N₄/WS₂ nanocomposite under influence of visible light.

References

- [1] Han, J., Bian, Y., Zheng, X., Sun, X., & Zhang, L. (2017). A photoelectrochemical cell for pollutant degradation and simultaneous H₂ generation. *Chinese Chemical Letters*, 28(12), 2239-2243.
- [2] Jo, W. K., Moru, S., & Tonda, S. (2020). Magnetically responsive SnFe₂O₄/g-C₃N₄ hybrid photocatalysts with remarkable visible-light-induced performance for degradation of environmentally hazardous substances and sustainable hydrogen production. *Applied Surface Science*, 506, 144939.
- [3] Wu, H., & Zhang, Z. (2011). Photoelectrochemical water splitting and simultaneous photoelectrocatalytic degradation of organic pollutant on highly smooth and ordered TiO₂ nanotube arrays. *Journal of Solid State Chemistry*, 184(12), 3202-3207.



- [4] Ding, F., Yang, D., Tong, Z., Nan, Y., Wang, Y., Zou, X., & Jiang, Z. (2017). Graphitic carbon nitride-based nanocomposites as visible-light driven photocatalysts for environmental purification. *Environmental Science: Nano*, 4(7), 1455-1469.
- [5] Xu, F., Mo, Z., Yan, J., Fu, J., Song, Y., El-Alami, W., ... & Xu, H. (2020). Nitrogen-rich graphitic carbon nitride nanotubes for photocatalytic hydrogen evolution with simultaneous contaminant degradation. *Journal of colloid and interface science*, 560, 555-564.
- [6] He, F., Wang, Z., Li, Y., Peng, S., & Liu, B. (2020). The nonmetal modulation of composition and morphology of g-C₃N₄-based photocatalysts. *Applied Catalysis B: Environmental*, 118828.
- [7] Zeng, P., Ji, X., Su, Z., & Zhang, S. (2018). WS₂/g-C₃N₄ composite as an efficient heterojunction photocatalyst for biocatalyzed artificial photosynthesis. *RSC advances*, 8(37), 20557-20567.
- [8] Akple, M. S., Low, J., Wageh, S., Al-Ghamdi, A. A., Yu, J., & Zhang, J. (2015). Enhanced visible light photocatalytic H₂-production of g-C₃N₄/WS₂ composite heterostructures. *Applied Surface Science*, 358, 196-203.
- [9] Ansari, M. Z., Ansari, S. A., Parveen, N., Cho, M. H., & Song, T. (2018). Lithium ion storage ability, supercapacitor electrode performance, and photocatalytic performance of tungsten disulfide nanosheets. *New Journal of Chemistry*, 42(8), 5859-5867.
- [10] Lin, D., Zhou, Y., Ye, X., & Zhu, M. (2020). Construction of sandwich structured photocatalyst using monolayer WS₂ embedded g-C₃N₄ for highly efficient H₂ production. *Ceramics International*, 46, 12933-12941.
- [11] Yan, X., Xia, M., Xu, B., Wei, J., Yang, B., & Yang, G. (2018). Fabrication of novel all-solid-state Z-scheme heterojunctions of 3DOM-WO₃/Pt coated by mono-or few-layered WS₂ for efficient photocatalytic decomposition performance in Vis-NIR region. *Applied Catalysis B: Environmental*, 232, 481-491.
- [12] Ding, J., Liu, Q., Zhang, Z., Liu, X., Zhao, J., Cheng, S., ... & Dai, W. L. (2015). Carbon nitride nanosheets decorated with WO₃ nanorods: Ultrasonic-assisted facile synthesis and catalytic application in the green manufacture of dialdehydes. *Applied Catalysis B: Environmental*, 165, 511-518.
- [13] Zhou, Y., Ye, X., & Lin, D. (2019). One-pot synthesis of non-noble metal WS₂/g-C₃N₄ photocatalysts with enhanced photocatalytic hydrogen production. *International Journal of Hydrogen Energy*, 44(29), 14927-14937.